Cruise-Dash-Climb Analysis of an Airbreathing Missile

David F. Chichka*
Atlantic Research Corporation, Gainesville, Virginia
Uday J. Shankar*
RCA, Plainsboro, New Jersey
and
Eugene M. Cliff† and Henry J. Kelley‡
Virginia Polytechnic Institute and State University, Blacksburg, Virginia

The singular perturbation analysis method is applied to the determination of optimal range-fuel-time trajectories for an air-breathing missile. This method leads to the reduced-order "cruise-dash" model. Earlier work in this area is extended by the inclusion of two not-heretofore-considered limits on the dynamical system. The results of the earlier work are shown to hold throughout much of the velocity regime in which the missile operates, but operation in the very-high- and very-low-velocity ranges is shown to be sharply curtailed, with the operating points being changed drastically in some cases. Also, the effect of the nonzero minimum admissible throttle setting and resultant throttle chattering on the solution of the control problem is examined in some detail. Energy transients are examined.

Nomenclature

C_N	= normal force coefficient
C_X	= axial force coefficient
D	= drag
E	= energy height
g	= acceleration due to gravity
H	= Hamiltonian
H^0, H^1, H^2	= parts of the Hamiltonian
h	= altitude
J	= performance index
L	= lift
M	= Mach number
Q	= fuel flow rate
R	= range
T	= thrust
t	= time
V	= velocity
W	= weight
α	= angle of attack
β	= constraint
γ	= flight path angle
ϵ^1, ϵ^2, ϵ^3	= perturbation parameters
η	= throttle setting
λ_x	= costate variable
μ_x	= weight in performance index
ψ	= end condition

Superscripts

$\cdot$	= time derivative
$'$	= stretched-time derivative
$-$	= specified
$*$	= optimal

Subscripts

c	= chattering
e	= equilibrium
eo	= engine-out
F	= fuel
f	= final
T	= time, terrain

Presented as Paper 87-2512 at the AIAA Guidance, Navigation, and Control Conference, Monterey, CA, Aug. 17-19, 1987; received Sept. 8, 1987; revision received April 25, 1988.

*Systems Analyst. Member AIAA.
†Professor, Aerospace and Ocean Engineering Department. Member AIAA.
‡Christopher Kraft Professor, Aerospace and Ocean Engineering Department. Fellow AIAA.

Introduction

ADVANCED missile technology featuring throttleable airbreathing engines is attractive for long-range interception of airborne targets. The task of making efficient use of the throttle capability presents challenging problems to the flight-control designer and to the combat-systems analyst. New flexibility introduced by throttle control allows for a trade-off of range against time of flight. In general, one expects to achieve more range at lower speeds than at higher speeds. The fire-control system should have an estimate of the missile range/speed capability and could then select an appropriate average speed based on the target information and the exigency of the current situation. This selection would be supplied to the missile, perhaps as part of the prelaunch initialization.

In principle, of course, information could be transmitted to the missile in flight depending, in part, on the autonomy afforded the missile. Indeed, the fire-control system may wish to change the speed/range selection while the missile is still in flight, as new target data become available. Whatever the details of this fire-control procedure, it is clear that one needs an estimate of the range/speed capabilities of the missile as well as a missile controller configured to achieve any of the range/speed combinations selected.

Given these requirements it is of interest to seek the maximum range for a given average speed. If one can determine the maximum range, and characterize the flight control to achieve this range, then the missilery will be used in an optimum way. The system will then be able to achieve interceptions that other designers could not. This paper summarizes a preliminary study of optimal time-fuel-range trajectories for a Scramjet-powered missile.

Problem Statement

There are several ways of specifying the cost function to be minimized and the end conditions to be met. In this paper, the cost index is a weighted sum of elapsed time and range, while

the end condition requires that a specified amount of fuel be used:

$$J = \mu_T t_f - \mu_R R(tf) \tag{1a}$$

subject to

$$\psi = W_F = (t) - W_{Ff} = 0 \tag{1b}$$

One might invoke *Meyer reciprocity* (see Ref. 1 for a discussion of the finite-dimensional case) to construct other "equivalent" problems. In Eqs. (1) the weights μ_T and μ_R are specified nonnegative constants and W_{Ff} is a specified amount of fuel to be used.

Problem Formulation

The dynamical system considered here is a point-mass missile model of vertical-plane motions. Rigid-body motions as well as structural vibrations are ignored. Also, the thrust is along the path and the weight of the missile is assumed to be constant. An appropriate set of equations is

$$\dot{h} = V \sin\gamma \tag{2a}$$

$$\dot{\gamma} = g/V\,[(L/W) - \cos\gamma] \tag{2b}$$

$$\dot{E} = [(T - D)/W]V \tag{2c}$$

$$\dot{R} = V \cos\gamma \tag{2d}$$

$$\dot{W}_F = Q \tag{2e}$$

where $V = \sqrt{2g(E - h)}$ and subject to the constraints:

$$\beta_1 = (h - h_T) \quad \geq 0 \quad \text{(terrain limit)} \tag{3a}$$

$$\beta_2 = (\alpha_{\max} - \alpha) \quad \geq 0 \quad \text{(aerodynamic limit)} \tag{3b}$$

$$\beta_3 = h - \bar{h}(M) \quad \geq 0 \quad \text{(Mach altitude limit)} \tag{3c}$$

$$\beta_4 = \eta_{\max}(h,M) - \eta \quad \geq 0 \quad \text{(propulsive limit)} \tag{3d}$$

Note that the constraint form β_3 could apply to a dynamic pressure limit or to a stagnation pressure limit. The constraint form β_4 reflects a *thermal choke limit*. This constant arises because of an upper bound on heat addition possible while maintaining a steady flow through the engine.[2] The state variables are h,γ,E,R, and W_F. The controls are α and η. The task is to determine $\alpha(\cdot)$ and $\eta(\cdot)$, to minimize the cost function.

While the optimal-control problem as stated may be approached in several ways, the need for closed-loop *synthesis* forces one to seek simplifications. The approach taken here is to reduce the order of the model by employing the singular perturbation theory (SPT).[3-6] This reduction is possible, because the relative response speeds of the states are different. Introducing interpolation parameters by way of SPT, the system equations are now written

$$\epsilon^2\dot{h} = V \sin\gamma \tag{4a}$$

$$\epsilon^2\dot{\gamma} = g/V\,[(L/W) - \cos\gamma] \tag{4b}$$

$$\epsilon^1\dot{E} = [(T - D)/W]V \tag{4c}$$

$$\dot{R} = V \cos\gamma \tag{4d}$$

$$\dot{W}_F = Q \tag{4e}$$

Note that by setting ϵ^2 or ϵ^1 to zero the order of the system is reduced. Before the solution of the problem is attempted, the aerodynamic and propulsive model is discussed.

Aerodynamic and Propulsive Models

The principal aerodynamic data is specified in terms of normal- and axial-force coefficients C_N and C_x. The normal-force coefficient is represented as a function of angle of attack α and Mach number M by cubic spline-lattice interpolation. It is noted that for a given Mach number, the coefficient C_N is nearly a linear function of α. The axial-force coefficient is dependent on M, α, and the altitude h. Since three-variable splines are computationally undesirable, the axial-force coefficient is approximated as a quadratic in α with the coefficients represented by cubic spline-lattice interpolation in M and h. The missile configuration under study is symmetric about the x-y plane and so the slope of C_x vs α is zero at the origin. Thus, the form is

$$C_x(M,h,\alpha) = a_0(M,h) + a_2(M,h) \cdot \alpha^2 \tag{5}$$

The propulsive model of the Scramjet engine is complex by the usual standards of performance optimization. Briefly stated, the airflow (mass rate) is calculated as

$$W_a = \rho V S_e A(M) \tag{6}$$

where S_e is the constant inlet area and $A(\cdot)$ is a Mach-dependent "capture ratio." More complicated dependencies, for example $A(M,\alpha)$, are possible. Associated with a given airflow is a fuel rate for perfect (stochiometric) combustion Q_s. For a given atmospheric model it is seen that Q_s is a function of M and h. The throttle setting η is defined as the fraction of stochiometric flow; that is

$$Q(M,h,\eta) = \eta Q_s(M,h) \tag{7}$$

The throttle setting is subjected to several limitations. There is a value of η (positive and fixed) below which the engine will not operate. The maximum value of η is nominally unity; however this is subjected to two further limitations. The first of these is a limit on the maximum fuel flow rate and the second is the thermal choke limit mentioned earlier. The latter is a function of M and h and is represented as a cubic spline lattice.

With the fuel flow now determined, the amount of thrust generated by the engine is given by

$$T(M,h,\eta) = Q(M,h,\eta) I_{sp}(M,h,\eta) \tag{8}$$

The specific impulse I_{sp} is represented by cubic spline-lattice interpolation as a function of M and *h for each throttle setting* in a given collection $\{\eta_j\}$. The emerging values are fitted by a quadratic in η (least squares) so that

$$I_{sp}(M,h,\eta) = w_1(M,h) + w_2(M,h)\eta + w_3(M,h)\eta^2 \tag{9}$$

It is important to note that these fits must be examined for the "correct" curvature. In terms of a thrust vs fuel flow plot (for fixed M and h) the curvature should be downward ($\partial^2 T/\partial Q^2 < 0$). If this were not so, then "chattering" throttle operation would likely arise.[7] Finally, the engine inlet is responsible for an increment in axial drag. This incremental coefficient is represented as a function of M by cubic spline interpolation.

Order Reduction

To "solve" the problem, one proceeds to form the variational Hamiltonian. We consider the performance index in Lagrange form (see Ref. 8, pp. 71 ff). Due to the explicit

time scaling in Eqs. (4), it is convenient to compose the Hamiltonian in several pieces.

$$H^0 = \lambda_F Q - \lambda_R V \cos\gamma \tag{10a}$$

$$H^1 = \lambda_E[(T-D)/W]V \tag{10b}$$

$$H^2 = \lambda_h V\sin\gamma + \{\lambda_\gamma(g/V)[(L/W) - \cos\gamma]\} \tag{10c}$$

The Hamiltonian of the system is

$$H = H^0 + \frac{H^1}{\epsilon^1} + \frac{H^2}{\epsilon^2} \tag{11}$$

The costates λ satisfy the adjoint differential equations

$$\dot{\lambda}_i = -\frac{\partial H}{\partial x_i} \tag{12}$$

where x_i is one of the states: h,γ,E,R, and W_F. It is appropriate to consider a change of variables suggested by the asymptotic structure. If, for example, one were to consider the problem with $\epsilon^2 = 0$, then the corresponding right members of Eqs. (4) would be algebraic constraints. These can be handled by adjoining them with "multipliers" such as $\tilde{\lambda}_h$ and $\tilde{\lambda}_\gamma$. A formal comparison of the necessary conditions of both problems ($\epsilon^2 = 0$ and $\epsilon^2 \neq 0$) suggests that:

$$\lim_{\epsilon^2\to 0} \frac{\lambda_h}{\epsilon^2} = \tilde{\lambda}_h \tag{13a}$$

$$\lim_{\epsilon^2\to 0} \frac{\lambda_\gamma}{\epsilon^2} = \tilde{\lambda}_\gamma \tag{13b}$$

One is led to "absorb" the ϵ^2 parameter in the adjoint variables and define

$$\tilde{\lambda}_h(t,\epsilon^2) \equiv [\lambda_h(t,\epsilon^2)]/\epsilon^2 \tag{14}$$

with a similar construction for $\tilde{\lambda}_\gamma$ and $\tilde{\lambda}_E$. In this formalism the ϵ^i factors are absorbed by the adjoints so that the pseudo-Hamiltonian is:

$$H = H^0 + H^1 + H^2 \tag{15}$$

The adjoint equations are now written

$$\epsilon^2\dot{\lambda}_h = -\frac{\partial H}{\partial h} \tag{16a}$$

$$\epsilon^2\dot{\lambda}_\gamma = -\frac{\partial H}{\partial \gamma} \tag{16b}$$

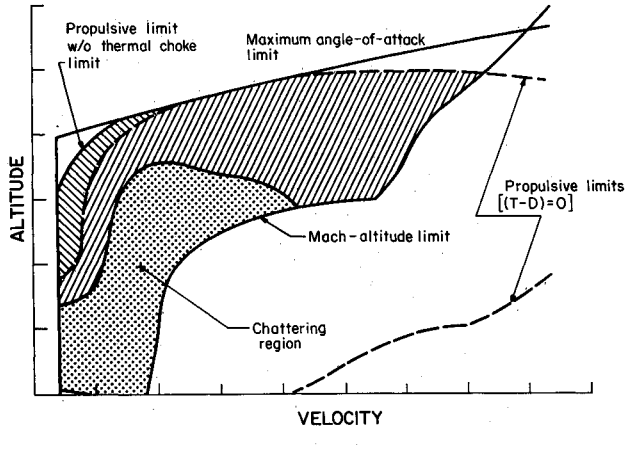

Fig. 1 Flight envelope.

$$\epsilon^1\dot{\lambda}_E = -\frac{\partial H}{\partial E} \tag{16c}$$

$$\dot{\lambda}_R = +\frac{\partial H}{\partial R} = 0 \tag{16d}$$

$$\dot{\lambda}_F = -\frac{\partial H}{\partial W_F} = 0 \tag{16e}$$

In these expressions, and in what follows, the tilde over the adjoints λ_h, λ_γ, and λ_E has been suppressed. The plus sign in the $\dot{\lambda}_R$ [Eq. (16d)] results from our choice to have λ_R positive and the explicit minus sign in H^0 [Eq. (10a)]. Considering the asymptotic behavior of the problem as ϵ^2 and ϵ^1 tend to zero leads to three subproblems. Two of these are treated in the following section.

Outer Solution – Cruise Dash

The first problem is extracted by considering $\epsilon^1 = \epsilon^2 = 0$. The order of the state is reduced to two. The remaining states are R and W_F. This problem is more fully considered in Ref. 9. However, the current model introduces new complexities, and to make the discussion complete, it is reiterated here. With $\epsilon^1 = \epsilon^2 = 0$, the first three equations are algebraic constraints, and one deduces that

$$\gamma = 0 \tag{17a}$$

$$L = W \tag{17b}$$

$$T = D \tag{17c}$$

For given values of h and E, which are now control variables, $L = W$ gives α and $T = D$ gives η. Since these conditions ensure that $H^1 = H^2 = 0$, the min H operation required by the minimum principle is the same as finding h and E to minimize H^0. As seen in Eqs. (16) the costates of R and W_f are constant. Also, since the system is autonomous, H = constant is a first integral of the system. The terminal transversality conditions require that

$$H^0(t_f) = -\mu_T \tag{18a}$$

$$\lambda_R = +\mu_R \tag{18b}$$

From these conditions one can solve for λ_F as

$$\lambda_F = [\mu_R V(t_f) - \mu_T]/[Q(t_f)] \tag{19}$$

The min H operation can be interpreted as seeking a point that minimizes the quantity

$$J = \lambda_F Q - \lambda_R V \tag{20}$$

subject to the aforementioned constraints. Thus, the "outer" cruise-dash problem amounts to finding a point in the altitude/airspeed chart that minimizes a weighted sum of fuel rate and range rate (speed) subject to the usual level-flight equilibrium conditions [Eqs. (17)]. The level-flight envelope for the vehicle under study is shown in Fig. 1. Note that the Mach altitude limit severely restricts the admissible operating points. The thermal choke limit has relatively little impact on the level-flight case: it limits high altitude operations only at relatively low speeds. The cross-hatched "chattering" region is the collection of points at which the level-flight drag is less than the minimum allowable thrust. Mathematically, unaccelerated flight in this region requires rapid switching between engine-out ($\eta = 0$) and an appropriate "low" thrust setting. Note that while such throttle chattering may strain the validity of the propulsive data, it is an inevitable mathematical

consequence of the nonconvexity of the thrust/fuel rate data.[7] In this sense, chattering controls are indicative of modeling weaknesses.

As noted in Ref. 9, the problem of minimizing J [Eq. (20)] is more easily analyzed by considering $\min_{h,V} J$ rather than $\min_{h,E} J$. One further notes that the minimizing operation can be carried out sequentially, i.e.,

$$\min_{h,V} J(h,V) = \min_{V} [\min_{h} J(h,V)] \tag{21}$$

and that the second term in the sum defining J does not depend on the variable h. It is useful to define $Q^*(V)$ by

$$Q^*(V) \equiv \min_{h} Q(h,V) \tag{22}$$

and note that

$$\min_{h} J(h,V) = \lambda_F Q^*(V) - \lambda_R V \tag{23}$$

Since Q^* is independent of λ_R and λ_F, one is led to the idea of constructing the Q^* curve in the Q-V plane. Once this is done, the velocity for which J is a minimum can be found for any specified λ_R and λ_F. From the definition of $Q^*(V)$, one can then extract the operating altitude.

The $Q^*(V)$ curve is generated by specifying V and performing a one-dimensional minimization of Q over h. The range of altitudes to be examined is defined by the constraints in (3). Two cases are presented here. The first, referred to as the "unconstrained case" uses only β_1 and β_2 to limit h; the other, "constrained" case, includes β_3 and β_4. The range of h is further limited by the propulsive limits shown in the flight envelope $[T - D \geq 0]$.

Once the range of altitudes has been determined, the minimization is carried out using a grid-search algorithm. This necessitates finding Q for several altitudes at each velocity. While conceptually straight forward, this is in practice somewhat intricate. A brief outline of the procedure is given here.

With the altitude and velocity specified, one recalls that C_N and C_x are defined as $C_N(M,\alpha)$ and $C_x(h,M,\alpha)$. This leads to searching over α until the requirement that lift equals the (known) weight is satisfied. With α known, the drag can be found.

Recalling that $T = \eta Q_s(M,h)\ I_{sp}(M,h,\eta)$, one notes that enough information is available to evaluate the throttle setting so that $T = D$. Since Q_s is fully specified by the altitude and velocity, it is only necessary to solve for η from

$$\eta Q_s(M,h)\ I_{sp}(M,h,\eta) = D \tag{24}$$

Noting that I_{sp} for a specified h and V is a quadratic in η, this amounts to finding the roots of a cubic. In general, only one of these roots is expected to fall in the range $[\eta_{\min}, \eta_{\max}]$, but it is mathematically possible that two, or all three, might. It is also possible that none of them will, particularly as the upper bound on the throttle is reduced from unity by the thermal choke limit β_4.

In addition to the roots of the cubic Eq. (24), the possibility of a chattering throttle setting as previously mentioned, must be considered. The calculation of such a setting is best described graphically, as in Fig. 2. A line drawn from the point $(0, -D_{eo})$ (where, D_{eo} refers to the drag evaluated at lift-equals-weight and engine-out) to any point on the $T(\eta) - D$ curve for which $(T - D > 0)$ must cross the $(T - D = 0)$ line. This point of intersection is a chattering setting. In those cases, where thrust exceeds drag for all throttle settings above $\eta_{\min}$, this setting is the only way in which "steady" flight can be achieved.

As the minimum value of Q is sought, (recall that Q is a monotone function of η for a fixed h and E), only the minimum value of η where $(T - D = 0)$ is of interest. Thus,

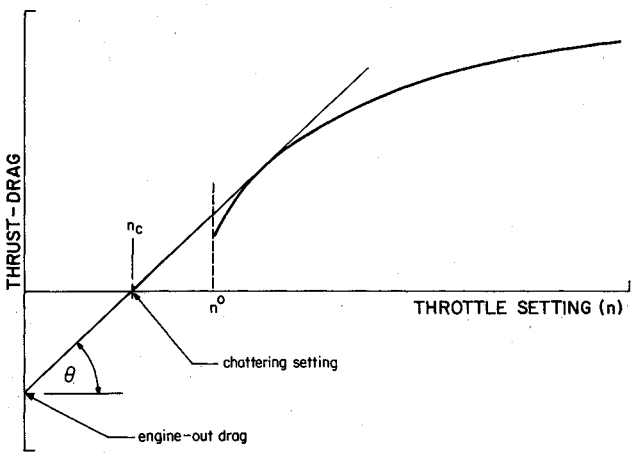

Fig. 2 Chattering cruise throttle setting.

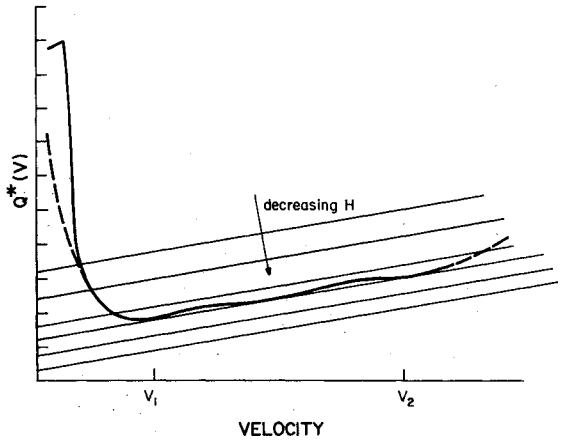

Fig. 3 Minimum fuel flow rate at cruise.

one imagines constructing the family of straight lines from $(0, -D_{eo})$ to points on the $[\eta, T(\eta) - D]$ curve. Among all such lines find the one that intersects the horizontal axes $(T - D = 0)$ at the smallest η. This is the best chattering solution and it must be considered along with the solutions of the cubic Eq. (24). In the model used in this study, chattering throttle values were not found to be optimal for any of the maneuvers studied. If the configuration had been exceptionally "clean" in the engine-out mode (low D_{eo}) then a chattering operation would arise.

Once the minimum useable value of η is found, Q is computed as before. The minimization algorithm continues, choosing new values of h until the lowest fuel flow has been found for the velocity being considered. This is Q^* at that V.

The $Q^*(V)$ curves for both the unconstrained (dashed line) and constrained (solid line) cases are shown in Fig. 3. One notes immediately that the curves are identical over most velocities. The difference at the lower end is because of the thermal choke limit; the optimal fuel flow for the unconstrained case requires a throttle setting above that allowed by this limit. At these low velocities the least fuel flow occurs at a much higher altitude for the unconstrained case than for the constrained case.

The difference in the curves at the high-velocity end is due to Mach altitude limit β_3. While the unconstrained curve continues into ever higher velocities, the constrained curve comes up against the limit and quickly reaches the outer bounds on the restricted flight envelope. Figure 4 shows the locus of constrained cruise altitudes in the altitude/airspeed chart. The usual limits are also shown.

The velocity that minimizes $J(V)$ depends on the ratio λ_R/λ_F. Lines of constant J can be drawn in the $Q - V$ plane as straight lines. The slope of these constant J lines is

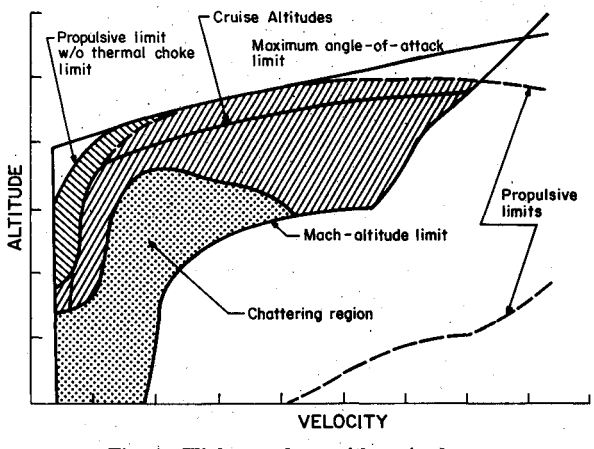

Fig. 4 Flight envelope with cruise locus.

$(-\lambda_R/\lambda_F)$. It is desired to find the line of constant J with the lowest value that intersects the $Q^*(V)$ curve. Should there be only one point of contact, this will be optimum, and the operating altitude and velocity will be unique.

Note that the slope of the constant J lines will always be non-negative. Thus, the optimum will always be some velocity equal to or greater than that at which the global minimum of $Q^*(V)$ occurs. As $|\lambda_R/\lambda_F|$ increases, the lines rotate counter clockwise, and the optimum moves to the right on the curve. As originally formulated, one imagines that the positive weights η_T and μ_F are given while the multipliers λ_R and λ_F are calculated. In fact it is computationally simpler to solve the problem (20) for a given (λ_R,λ_F) pair and then to use Eqs. (18) and (19) to find the associated weights μ_T and μ_R. As $|\lambda_R/\lambda_F|$ increases, one puts more emphasis on time, and as a result, the optimum velocity becomes higher.

At some values of λ_R/λ_F the situation shown in Fig. 3 occurs. In this figure, the slope of the constant J lines is such that both V_1 and V_2 result in the same minimum of J. For a lower $|\lambda_R/\lambda_F|$, the optimal velocity is less than V_1; for a greater $|\lambda_R/\lambda_F|$ the optimum is greater than V_2.

An important feature of Fig. 3 is that velocities in the range between V_1 and V_2 are *never* optimal (i.e. for no λ_R/λ_F ratio is such a velocity minimizing). Indeed, if one were required to achieve an average speed in the interval (V_1, V_2), the best program would involve operation for a while at $[h_c(V_1), V_1]$ followed by an operation at $[h_c(V_2), V_2]$, the time being apportioned so as to achieve the required average speed. Note that the cruise model gives no indication in what order these points should be flown. Further, note that on account of this nonconvexity, the notion of Meyer reciprocity, noted in the Problem Statement, must be used with considerable caution.

Energy Layer

Following the procedure in Kelley[5] the next step is to account approximately for the energy transient. This energy-layer analysis has been discussed in Refs. 10 and 11, albeit for a simpler propulsive model. The outer analysis suggests that there are two interesting "cruise" points. One of these is a "low-speed" point $[h_c(V_1), V_1]$, while the other is a "high-speed" point $[h_c(V_2), V_2]$. The cruise-dash model describes the transitions from an arbitrary initial energy to the first cruise-dash energy and from one cruise-dash energy to the other, as jump discontinuities. This is because energy is control-like in the outer layer.

To better approximate the energy transient, one introduces a time-stretching transformation $\tau = t/\epsilon^1$. To extract the zeroth order approximation one considers the limits $\epsilon^1 \to 0$ and $(\epsilon^2/\epsilon^1) \to 0$. The equations can then be written

$$(\epsilon^2/\epsilon^1)h' = V\sin\gamma = 0 \tag{25a}$$

$$(\epsilon^2/\epsilon^1)\gamma' = g/V[(L/W) - \cos\gamma] = 0 \tag{25b}$$

$$E' = [(T-D)/W]V \tag{25c}$$

$$R' = \epsilon^1 V\cos\gamma = 0 \tag{25d}$$

$$W_F' = \epsilon^1 Q = 0 \tag{25e}$$

with the costate equations

$$(\epsilon^2/\epsilon^1)\lambda_h' = -\frac{\partial H}{\partial h} = 0 \tag{26a}$$

$$(\epsilon^2/\epsilon^1)\lambda_\gamma' = -\frac{\partial H}{\partial \gamma} = 0 \tag{26b}$$

$$\lambda_E' = -\frac{\partial H}{\partial E} \tag{26c}$$

$$\lambda_R' = +\epsilon^1\frac{\partial H}{\partial R} = 0 \tag{26d}$$

$$\lambda_{W_F}' = -\epsilon^1\frac{\partial H}{\partial W_F} = 0 \tag{26e}$$

Equations (25a and (25b) require level flight ($\gamma = 0$, $L = W$). Equations (25d) and (25e) imply that the range and fuel flow are frozen in the boundary layer. These two variables are "ignorable" in any case.

The adjoint equations (26) indicate that h and γ are like control variables (and also that λ_R and λ_F are constant) in the boundary layer. The differential equation for λ_E can be written as

$$\lambda_E' = -\lambda_E\frac{\partial P_s}{\partial E} + \lambda_R\frac{\partial V}{\partial E} - \lambda_F\frac{\partial Q}{\partial E} \tag{27}$$

where P_s is the specific excess power $[(T-D)/W]V$ and drag is evaluated at lift-equals-weight. The controls h and η are chosen to minimize H. Analogous to the outer problem, H^2 is identically zero. The cost for the energy layer is now

$$J = \mu_T\tau_f + \lim_{\tau f\to\infty}\int_0^{\tau f}(\lambda_F Q - \lambda_R V)\mathrm{d}\xi \tag{28}$$

The pseudo-Hamiltonian is

$$H = -\lambda_R V + \lambda_F Q + \lambda_E P_s \tag{29}$$

One can find λ_E from the adjoint differential equation, but it is easier to use the first integral $H = -\mu_T$. The optimality conditions require that the optimal controls h and η minimize H, which is equivalent to minimizing $H + \mu_T$. Also, since E is constant, the minimization can be over h or V, and the minimum value of $\hat{H} \equiv H + \mu_T$ is zero.

To determine the character of this problem, let $u = \mathrm{col}(\eta, V)$ and consider

$$f(u) \equiv \lambda_F Q(\eta, V) + \mu_T - \lambda_R V \tag{30a}$$

$$g(u) \equiv P_s(\eta, V) \tag{30b}$$

Writing λ for λ_E, the problem is to

$$\min_u \hat{H}(u) = \min_u [f(u) + \lambda g(u)] \tag{31}$$

with the minimum value being zero.

Consider the (g, f) plane shown in Fig. 5. The admissible set of (g, f) is shaded. For $\lambda < 0$, lines of constant $\hat{H}$ have a positive slope and, since the minimum value of $\hat{H}$ must be zero, the "separating" line must go through the origin. For the illustrative case shown in Fig. 5, the extremal point is (g^*, f^*). Note that (g^*, f^*) maximizes the ratio (g/f), i.e., the

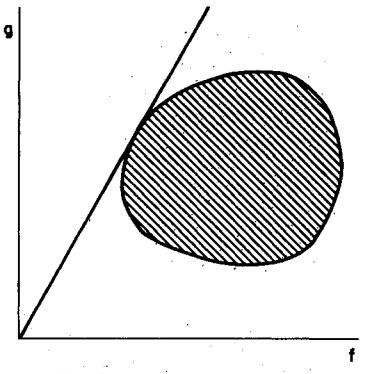

Fig. 5 Generic Hodograph.

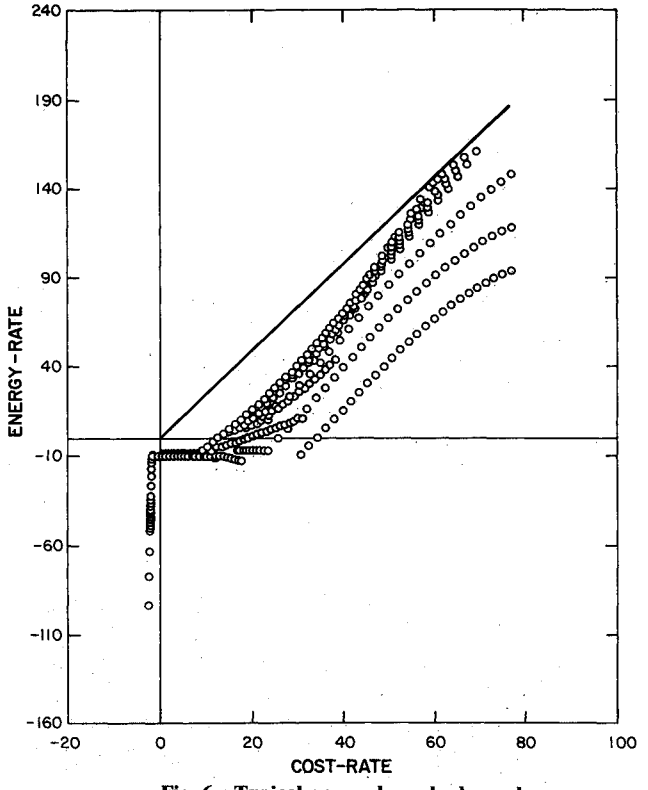

Fig. 6 Typical energy-layer hodegraph.

slope of a line joining the origin to a point in the admissible set. This is true for the case $\lambda<0$ considered here, *as long as the operating point is in the first quadrant.* For third-quadrant operation the extremal point *minimizes* the ratio (g/f). Trajectory segments with $\lambda<0$ would require purposeful energy dissipation and do not occur in the families of interest here. The fact that the solution to the minimization problem (31) furnishes a stationary value for the ratio (g/f) is established in Ref. 5 (the treatment in Ref. 5 requires certain smoothness assumptions on the functions f and g). Translating this analysis to the problem at hand, the task of minimizing the pseudo-Hamiltonian Eq. (29) is equivalent to:

$$\max_{\eta,V} \frac{P_s(\eta,V)}{\lambda_F Q(\eta,V) + \mu_T - \lambda_R V} \tag{32}$$

The multipliers λ_R, λ_F, and μ_T are known from the "outer" problem, while the energy is a parameter. In principle, one solves the problem (32) over the range of energies of interest and so determines a feedback law for the throttle setting and speed (or altitude) viz. $\eta^*(E)$ and $h^*(E)$. Several features tend to complicate this picture.

First, consider Fig. 6, which displays the relevant (g,f) hodograph for the vehicle under study at a particular energy. The "tail" in the third quadrant is the locus of engine-out operating points over a range of altitudes. Note that problem (32) has *two* "local" answers: one corresponding to first-quadrant (engine-on) operation, while the other is a third-quadrant (minimum power required, engine-out) point. Intuition suggests that the first-quadrant point is appropriate for energy-gaining trajectories, while the third-quadrant point would be employed for energy-losing trajectories. This blends nicely with the outer problem where two "interesting" cruise points were found.

Suppose, for example, that one decides to climb out to the high-speed point $[(h_c(V_2),V_2)$ with energy $E_2]$, cruise for a while, then slow to the low-speed point $[(h_c(V_1),V_1)$ with energy $E_1]$ and cruise until fuel exhaustion. The preceeding analysis suggests that one should increase energy from its initial value to E_2 using the first-quadrant commands $\eta^*_+(E),h^*_+(E)$. As $E\to E_2$, the throttle setting and altitude controls will tend to the cruise values at $(h_c(V_2),V_2)$. This is so because the g,f hodograph at the cruise energy E_2 (or E_1) will contain the origin in its boundary. That is, the "outer" cruise points are singular points for the system of differential equations describing the energy transient.

After cruising for a time at the high-speed point, a flight management system would select the third-quadrant commands $\eta^*_-(E),h^*_-(E)$. This would allow the energy to decrease to the low-speed cruise value E_1. Steady operation would continue at $(h_c(V_1),V_1)$ until the fuel was exhausted.

Note that in the intermediate energy layer, the "fast" variables are specified as "controls" $h=h^*(E)$ and $\gamma=0$. The asymptotic analysis can be carried to the next level. This is done in a companion paper. In Ref. 7 an ad-hoc scheme is used to produce a load-factor command suitable for use in the point-mass simulation model.

While the program of formally computing the energy-transient commands [e.g., $\eta^*_+(E)$, $h^*_+(E)$] has been carried out, there is a weakness in the modeling. An examination of the hodograph Fig. 6 reveals a lack of convexity in the first-quadrant part of the boundary. In this case, one is obligated to "relax" the problem before proceeding with a theory based on the usual necessary conditions.[7] The relaxation procedure produces a related *singular* optimal control problem; these problems are typically more difficult to analyze.

In this application the extremal points were found to lie on the naturally convex part of the hodograph. For other missiles this may not be the case. Solutions that involve chattering altitude in the energy transient may portend altitude ripples and throttle thrashing in the point-mass-modeled optimal-flight history. It is of future interest to compare point-mass and singular-perturbation results in such problems.

Conclusions

The application of a singular perturbation approach to time-range-fuel optimization of a high performance throttleable Scramjet missile has led to some insights. Cruise analysis suggests there are two interesting altitude/speed points. Range-time tradeoffs amount to apportioning flight time between these points. Energy-layer analysis provides a candidate procedure for implementing efficient climb-out and slow-down profiles. However, convexity troubles cast serious doubts on the *optimality* of these procedures. Additional theoretical work is needed to examine the convexity issue and its implications. Also of interest in applications is the extension to three-dimensional flight.

Acknowledgment

The support of the Naval Surface Weapons Center, Dahlgren, Virginia under Contracts N60921-C-A110 and N60921-85-C-A165 (Task 6) is gratefully acknowledged. This research was supported in part by DARPA under (ACMP) Contract F49620-87-C-0116.

References

[1]Hestenes, M. R., *Optimization Theory: The Finite Dimensional Case*, Wiley-Interscience, New York, 1975, p. 156.

[2]Shapiro, A. H., *The Dynamics and Thermodynamics of Compressible Fluid Flow*, Ronald, New York, 1953, pp. 201–203.

[3]Ardema, M. D., "Singular Perturbations in Flight Mechanics," NASA TM-X-62-380, 2nd rev., July 1977.

[4]Ashley, H., "Multiple Scaling in Flight Vehicle Dynamic Analysis – A Preliminary Look," AIAA Guidance, Control, and Flight Mechanics Conference, Huntsville, AL, 1967.

[5]Calise, A. J. and Moerder, D. D., "Singular Perturbation Techniques for Real Time Aircraft Trajectory Optimization and Control," NASA CR-3597, 1982.

[6]Kelley, H. J., "Aircraft Maneuver Optimization by Reduced Order Approximation," *Control and Dynamic Systems*, Vol. 10, edited by C. T. Leondes, Academic, New York, 1973, pp. 131–178.

[7]Marchal, C., "Chattering Arcs and Chattering Controls," *Journal of Optimization Theory and Applications*, Vol. 11, 1973, pp. 441–468.

[8]Leitmann, G., *An Introduction to Optimal Control*, McGraw-Hill, New York, 1966.

[9]Bilimoria, K. D., Cliff, E. M., and Kelley, H. J., "Classical and Neo-classical Cruise-Dash Optimization," *Journal of Aircraft*, Vol. 22, July 1985, pp. 555–560.

[10]Bryson, A. E., Desai, M. N., and Hoffman, K., "Energy-State Approximation in Performance Optimization of Supersonic Aircraft," *Journal of Aircraft*, Vol. 6, Nov.-Dec. 1969, pp. 481–488.

[11]Glaros, L. N. and Crigler, S. W., "Real-Time Trajectory Control Using Augmented Energy Management," AIAA Paper 77-1052, 1977.